Examining the effects of anthropogenic emissions on isoprene-derived secondary organic aerosol formation during the 2013 southern oxidant and eerosol study (SOAS) at the Look Rock, Tennessee ground site

S. H. Budisulistiorini, X. Li, S. T. Bairai, J. Renfro, Y. Liu, Y. J. Liu, K. A. McKinney, S. T. Martin, V. F. McNeill, H. O. T. Pye, A. Nenes, M. E. Neff, E. A. Stone, S. Mueller, Christoph Knote, S. L. Shaw, Z. Zhang, A. Gold, J. D. Surratt

Angaben zur Veröffentlichung / Publication details:

Budisulistiorini, S. H., X. Li, S. T. Bairai, J. Renfro, Y. Liu, Y. J. Liu, K. A. McKinney, et al. 2015. "Examining the effects of anthropogenic emissions on isoprene-derived secondary organic aerosol formation during the 2013 southern oxidant and eerosol study (SOAS) at the Look Rock, Tennessee ground site." *Atmospheric Chemistry and Physics* 15 (15): 8871–88. https://doi.org/10.5194/acp-15-8871-2015.

Supplement of Atmos. Chem. Phys., 15, 8871–8888, 2015
http://www.atmos-chem-phys.net/15/8871/2015/
doi:10.5194/acp-15-8871-2015-supplement

Atmospheric Chemistry and Physics Open Access

Supplement of

Examining the effects of anthropogenic emissions on isoprene-derived secondary organic aerosol formation during the 2013 Southern Oxidant and Aerosol Study (SOAS) at the Look Rock, Tennessee ground site

S. H. Budisulistiorini et al.

Correspondence to: J. D. Surratt (surratt@unc.edu)

A. Sampling Site Location: Look Rock, Tennessee, USA

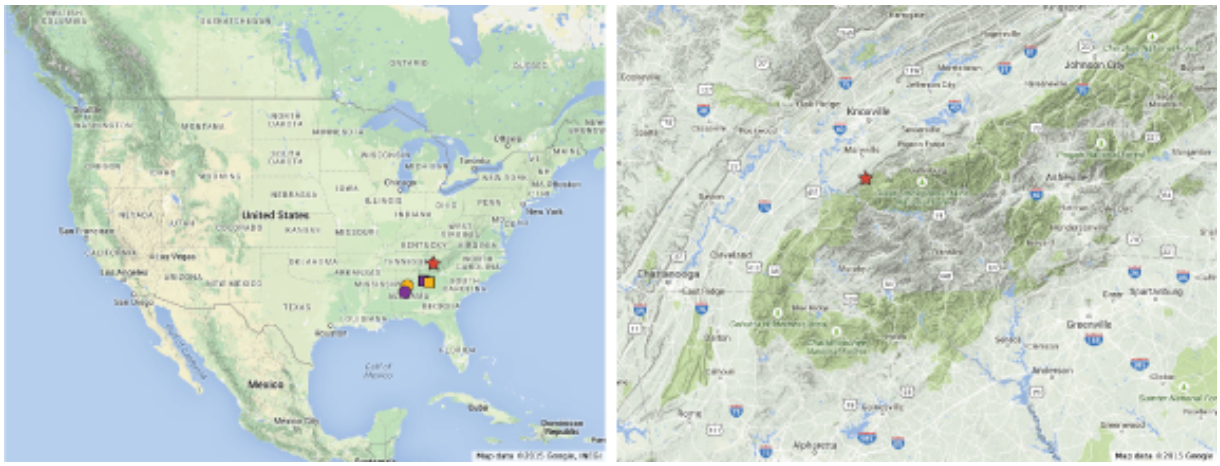

Figure S1. Maps of (a) United State of America, and (b) location of Look Rock, TN, (LRK) site. Courtesy by Google Maps.

The sampling site was located in Look Rock (LRK) site, Tennessee, USA, as marked in red star on left-panel Fig. S1. The circle marks are the other sampling sites participated in 2013 SOAS study located in Alabama, namely Centerville (purple) and Birmingham (yellow). The squares mark previous ambient aerosol measurements studies located in Atlanta, Georgia (yellow; Budisulistiorini et al., 2013) and Yorkville, Georgia (purple; Lin et al., 2013).

The right-panel of Fig. S1 illustrates area surrounding the LRK site. Knoxville, Maryville, Nashville, and Chattanooga urban areas are on the north to west of the site. The forested area of Great Smoky Mountains is stretched out from the northeast to the southwest of the site. As illustrated on Fig. S2, during the entire field campaign, the wind is coming mostly from the south and southeast of the site, as well as from the west. This would allow isoprene emitted from the forested area to be mixed with anthropogenic emissions from the urban areas. However, as the site is located at high elevation (~ 800 m above sea level), it is less likely that fresh emission could reach the site.

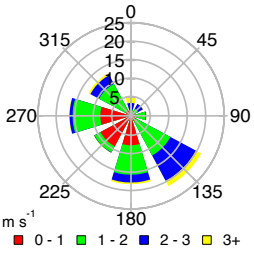

Figure S2. Wind direction at sampling location

B. Ambient PM_1 and Collocated Measurements

Table S1. Collocated gas- and particle-phase measurements at LRK site.

Compound	Instrument	Analysis Method	Reporting Frequency
SO_2	Thermo Scientific 43i TLE	Pulsed fluorescence	1 hr
CO	Thermo Scientific 48i TLE	NDIR-GFC	1 hr
NO	Thermo Scientific 42c	Chemiluminescence	1 hr
NO_y	Thermo Scientific 42c	Chem./Mo converter	1 hr
NO_2	API 200EU	Chem./photolytic conv.	1 hr
BC	Magee AE 22	Optical absorption	1 hr
SO_4	Thermo Scientific 5020	Thermal/fluorescence	1 hr
$PM_{2.5}$	Met One BAM-1020	Beta attenuation	1 hr
PM_{10}	Met One BAM-1020	Beta attenuation	1 hr
O_3[a]	Thermo Scientific 49i	UV absorption	1 hr

[a]Ozone is measured at National Park Service shelter next to LRK shelter

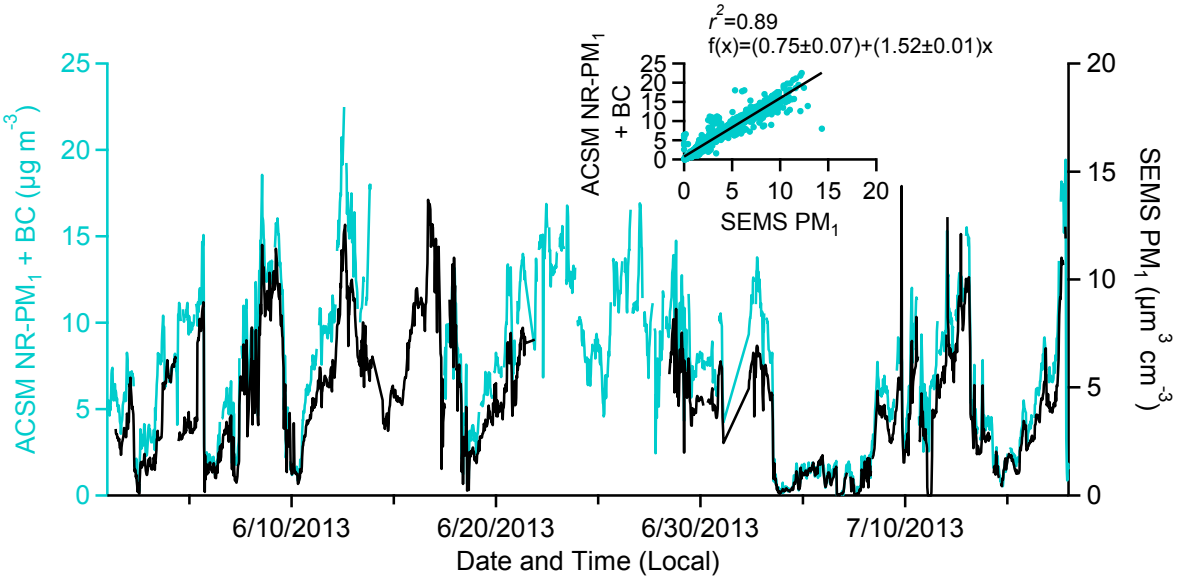

Figure S3. Comparison of PM_1 mass concentration from ACSM and black carbon measurements with PM_1 volume concentration from SEMS suggests a strong correlation. Slope shown in insert suggests an estimated aerosol density of 1.52 g cm^{-3}.

C. PMF Analysis

Table S2. Summary of PMF solutions obtained for 2013 SOAS campaign dataset.

# Factors	FPEAK	SEED	$Q/Q_{expected}$	Solution Description
1	0	0	0.27262	One-factor (OOA) resulted in large residuals at some time periods and *m/z*'s.
2	0	0	0.23717	Two-factor (IEPOX-OA and LV-OOA) is significantly reduced residuals. LV-OOA factor time trends and mass spectrum seem to be a mixture of less- and more-oxidized OA.
3	0	0	0.21338	Three-factor (IEPOX-OA, LV-OOA, and 91Fac) seems like an optimum solution. The 91Fac appears to share some similarities in time trend and mass spectrum to IEPOX-OA and LV-OOA but with a distinct *m/z* 91.
3	-0.2 to 0.2	0	0.2134-0.21447	In this range, factor mass spectra and time series are changing suggesting possibility of optimum solution.
3	**-0.09**	**0**	**0.2137**	**Optimum number of factors (IEPOX-OA, LV-OOA, and 91Fac) and FPEAK. All three factors have distinctive time trends and mass spectra, and compare well with independent particle and/or gaseous measurements, and reference mass spectra from database and/or experiment in this study.**
3	0	0-100 in steps of 5	0.21336-0.21353	For 3-factor, time trends and mass spectra are nearly identical at different starting points.
4 to 10	0	0	0.19965-0.16295	Q/Q_{exp} is reduced but OOA factor is split into more factors that do not compare well with reference mass spectra.

Table S3. Correlation of PMF 2-, 3-, and 4-factor solutions at Fpeak 0 with collocated measurements and reference mass spectra.

	2-factor		3-factor			4-factor			
	Fac1	Fac2	Fac1	Fac2	Fac3	Fac1	Fac2	Fac3	Fac4
r^2 *Time Series*									
CO	0.41	0.33	0.37	0.44	0.28	0.37	0.45	0.34	0.29
NO_x (=NO+NO_2)	0.02	0.01	0.03	0.01	0.02	0.03	0.01	0.00	0.05
NO_y	0.15	0.22	0.14	0.21	0.20	0.13	0.22	0.17	0.22
NO_z	0.15	0.22	0.14	0.21	0.21	0.13	0.21	0.17	0.23

	2-factor		3-factor			4-factor			
	Fac1	Fac2	Fac1	Fac2	Fac3	Fac1	Fac2	Fac3	Fac4
O_x (=NO_2+O_3)	0.18	0.21	0.15	0.30	0.13	0.14	0.32	0.16	0.16
SO4	0.37	0.16	0.35	0.31	0.14	0.35	0.33	0.19	0.17
ACSM SO_4	0.62	0.34	0.59	0.53	0.31	0.59	0.55	0.39	0.33
ACSM NO_3	0.75	0.73	0.72	0.80	0.70	0.70	0.79	0.74	0.68
ACSM NH_4	0.61	0.41	0.57	0.59	0.36	0.57	0.61	0.44	0.37
r^2 *Mass Spectra*									
HOA	0.11	0.05	0.17	0.03	0.57	0.18	0.02	0.35	0.29
LV-OOA	0.97	0.97	0.83	0.93	0.32	0.80	0.91	0.67	0.52
SV-OOA	0.55	0.41	0.64	0.32	0.88	0.64	0.28	0.91	0.44
BBOA	0.46	0.28	0.64	0.20	0.69	0.66	0.17	0.69	0.34
82Fac	0.89	0.71	0.94	0.60	0.47	0.94	0.56	0.68	0.38
91Fac	0.54	0.42	0.60	0.32	0.80	0.58	0.27	0.67	0.69
IEPOX-OA	0.81	0.65	0.89	0.56	0.53	0.89	0.52	0.84	0.33
Lab IEPOX SOA	0.55	0.32	0.80	0.24	0.38	0.83	0.21	0.53	0.19

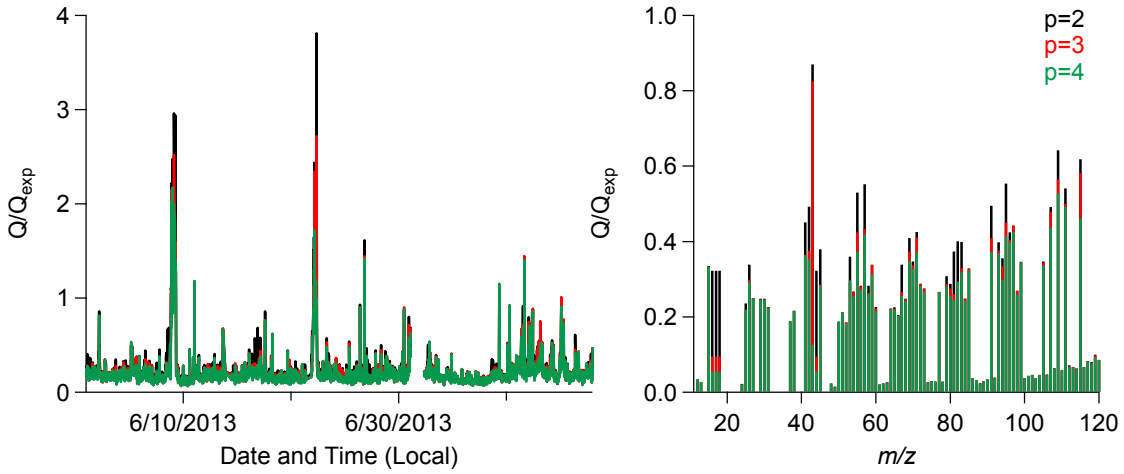

Figure S4. Time series and mass spectra of Q/Q_{exp} for 2-,3-, and 4-factor solutions are used to determine the optimum number of factor in PMF analysis. The 3-factor solution time series and mass spectra of Q/Q_{exp} suggest that adding the third factor reduces Q/Q_{exp} substantially. The 4-factor solution does not significantly reduce time series and mass spectrum of Q/Q_{exp} compared to those of 3-factor solution.

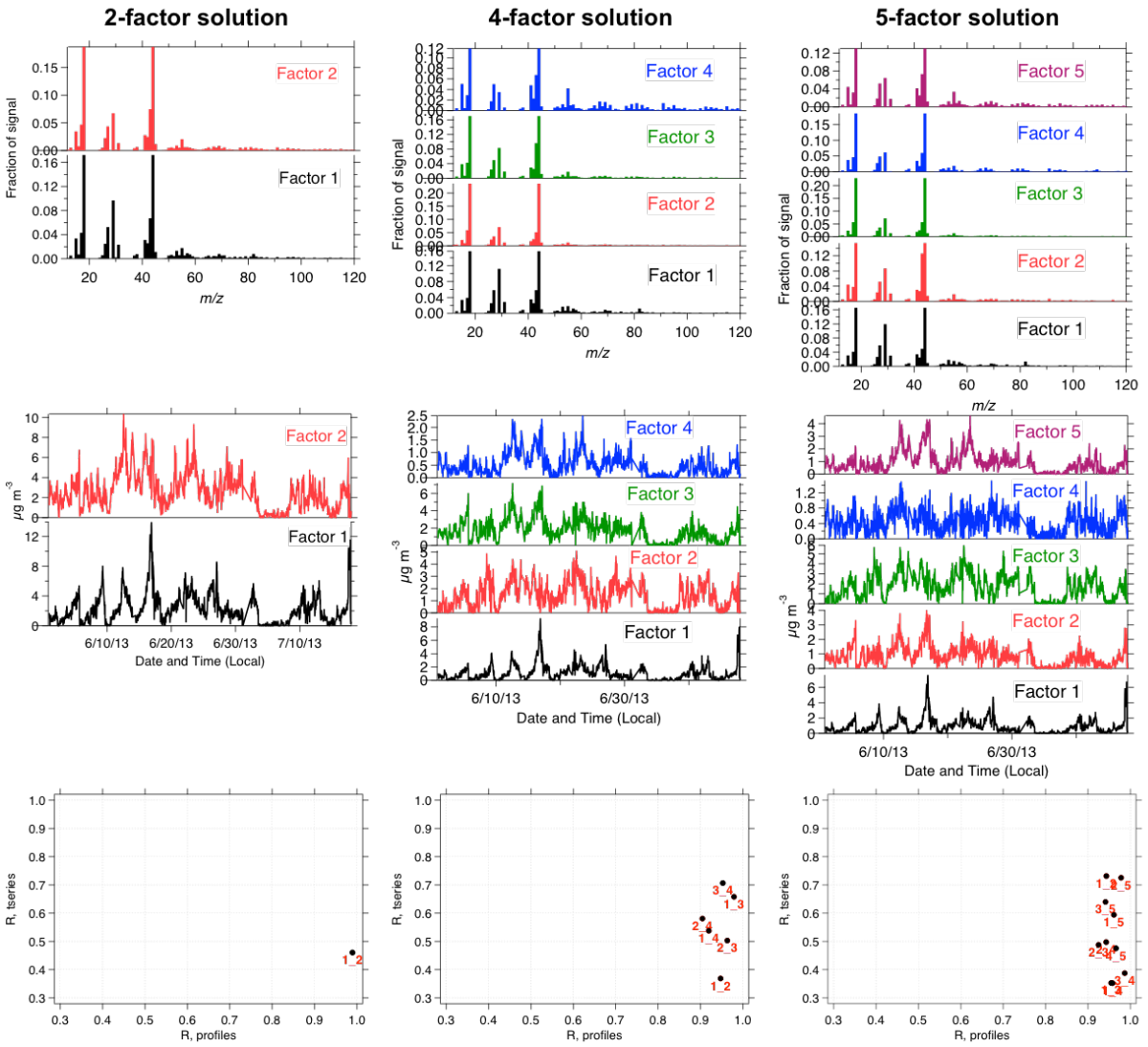

Figure S5. Time series, mass spectra, and factor correlation plots for 2-, 4-, and 5-factor solutions.

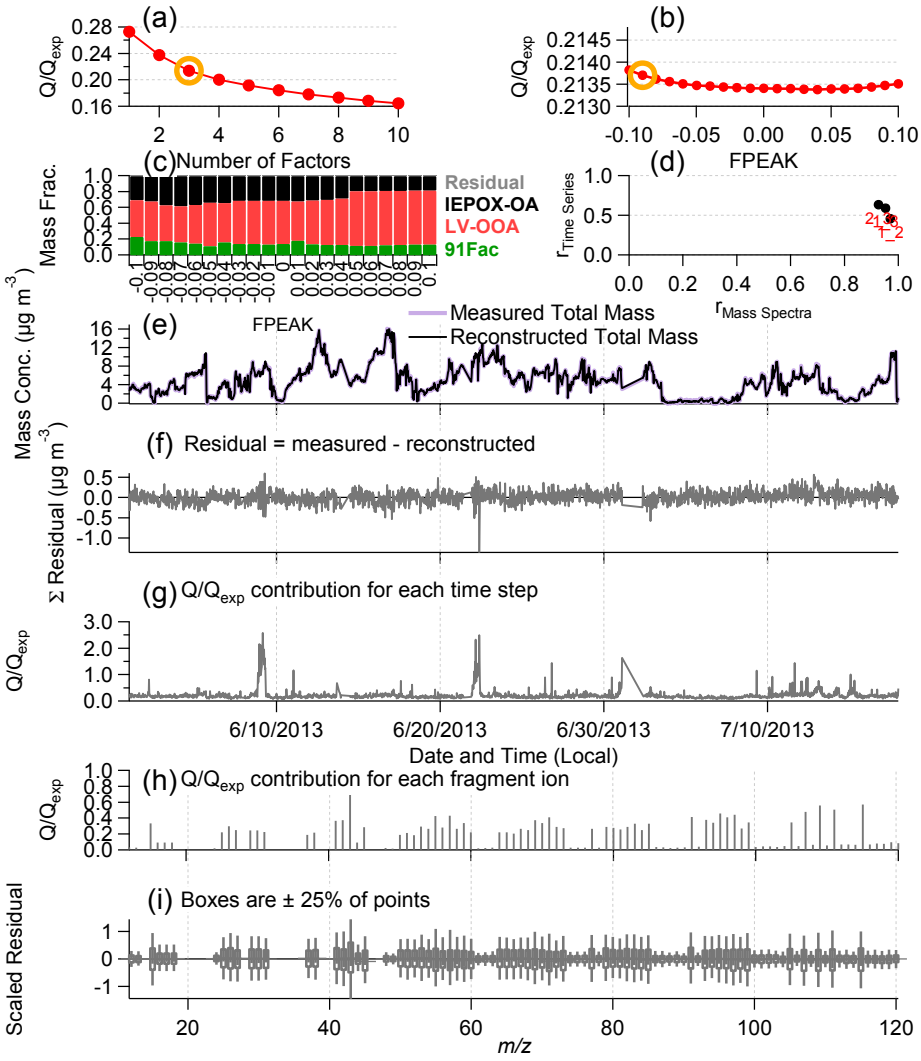

Figure S6. Diagnostic plots for 3 factor solution resolved from 2013 SOAS campaign dataset: (a) Q/Q_{exp} as a function of number of factors (p), (b) Q/Q_{exp} as a function of FPEAK selected for the chosen number of factors, (c) fractional contribution of OA factors for each FPEAK, (d) correlation among PMF factors based on factor time series and mass spectra, (e) TS of the measured OA mass and the reconstructed OA mass, (f) variation of the residual of the fit, Q/Q_{exp} for each point in time (g) and for each *m/z* (h), and the box and whisker plot of the scaled residuals for each *m/z*.

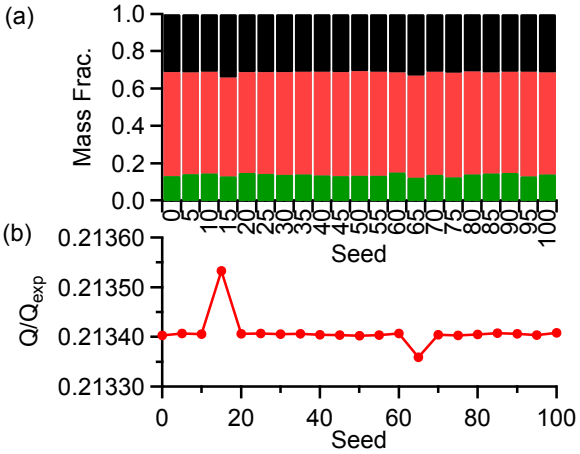

Figure S7. Diagnostic plots for seed analysis of PMF three factor solution: (a) fractional contribution of OA factors for each seed, and (b) Q/Q_{exp} as a function of seed selected for the chosen number of factors. Changes in mass fraction contribution of each factor are negligible (< 1%) over seed range. Similarly, *Q/Qexp* values at different seed are nearly identical with very small changes (< 1%).

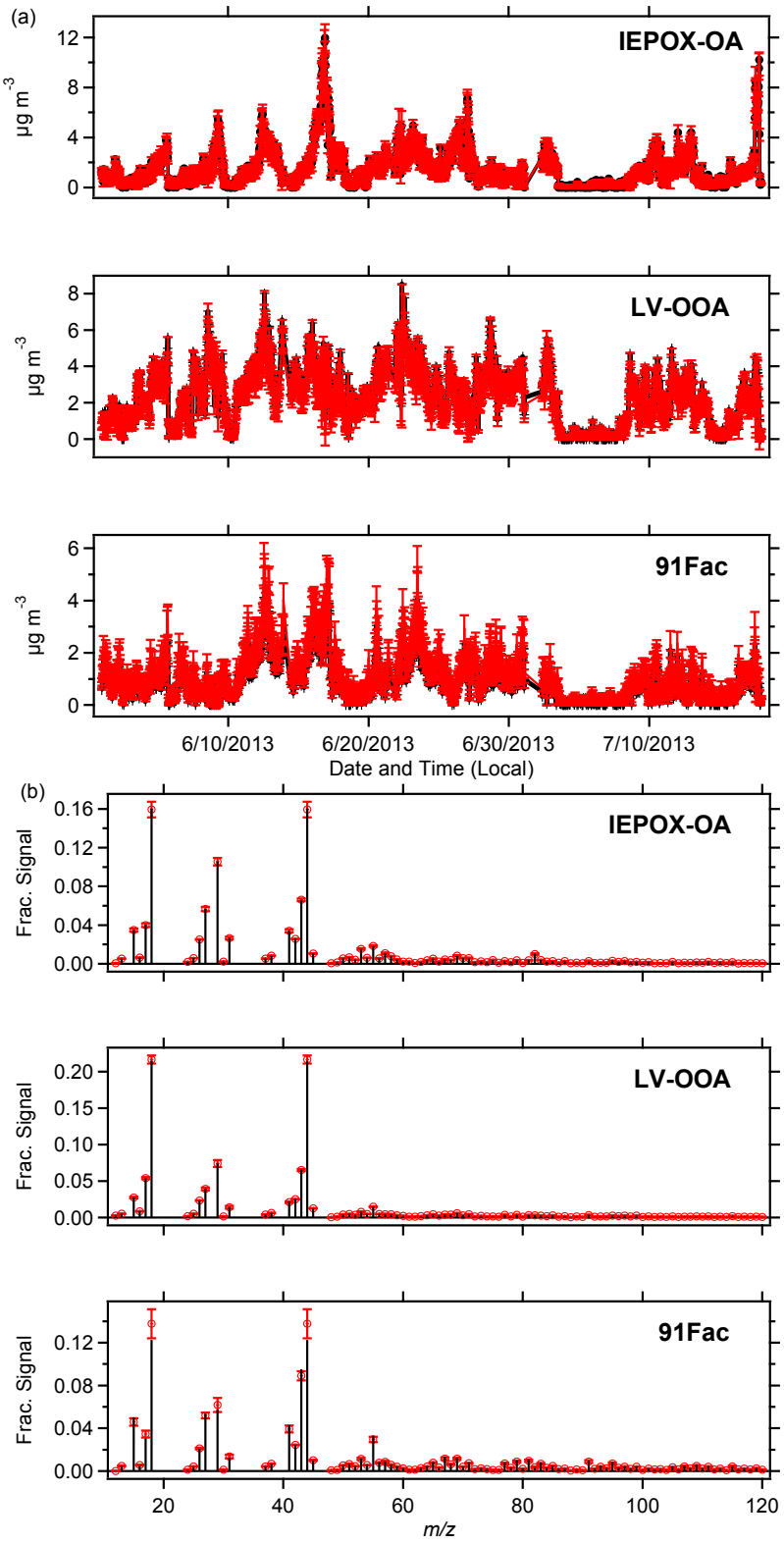

Figure S8. Results from bootstrapping analysis of the three factor solution of the 2013 SOAS campaign dataset. Average (a) time series and (b) mass spectra are shown in black with 1-σ error bars in red. All four factors show some uncertainty in their mass spectra and time series, which are nonetheless small compared to the general factor profile and contribution.

D. Filter Sampling Methods and Analysis

FLEXPART Model

The intensive filter sampling periods were selected on the basis of the FLEXPART Lagrangian particle dispersion model v. 9.02 (Stohl et al., 2005), driven by analytical data (every 6 hours) and 3 hour forecasts of the Global Forecast System (GFS) of the National Centers for Environmental Prediction (NCEP). Back-trajectory calculations were conducted on a 0.1 x 0.1 degree grid by releasing 10000 air parcels every 3 hours at each SAS field site and following parcels back in time for 72 hours. The resulting 3-hour surface residence time fields (concentration of parcels at a given time between 0 and 100 m above ground) were convolved with emission inventories and then spatially integrated to estimate total emissions injected into the air parcel during each 3-hour interval. This allowed estimation of (1) total emissions load of an air mass sampled at LRK (as well as the other ground sites), (2) the mixture of different emission source types (mobile, biogenic VOCs, biomass burning, etc.), and (3) the age (and hence amount of chemical processing) emissions experienced prior to arrival at LRK. NO_x and SO_2 concentrations were estimated from the National Emission Inventory (NEI), biomass burning emissions from the Fire Inventory from NCAR (FINN, Wiedinmyer et al., 2011) and biogenic VOC emissions were based on results of a MOZART global model (Emmons et al., 2010) simulation using the Model of Emissions of Gases and Aerosols from Nature (MEGAN, Guenther et al., 2006).

Filter Analysis

Table S4. Temperature program and purge gas type used in OC/EC analysis of particle-laden filter punches.

Step	Gas	Hold time (s)	Temperature (°C)
1	He	60	310
2	He	60	480
3	He	60	615
4	He	90	900
5	He	30	Oven off
6	He	8	550
7	He/O_2	35	600
8	He/O_2	45	675
9	He/O_2	45	750
10	He/O_2	45	825
11	He/O_2	120	920

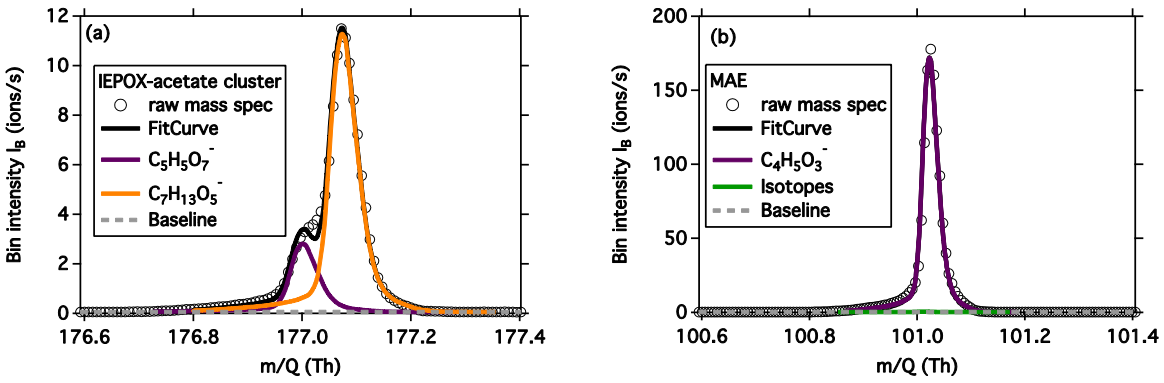

Figure S9. Typical high-resolution fitting of (a) IEPOX as an acetate cluster, and (b) MAE as a deprotonated ion from HR-ToF-CIMS measurement at LRK site.

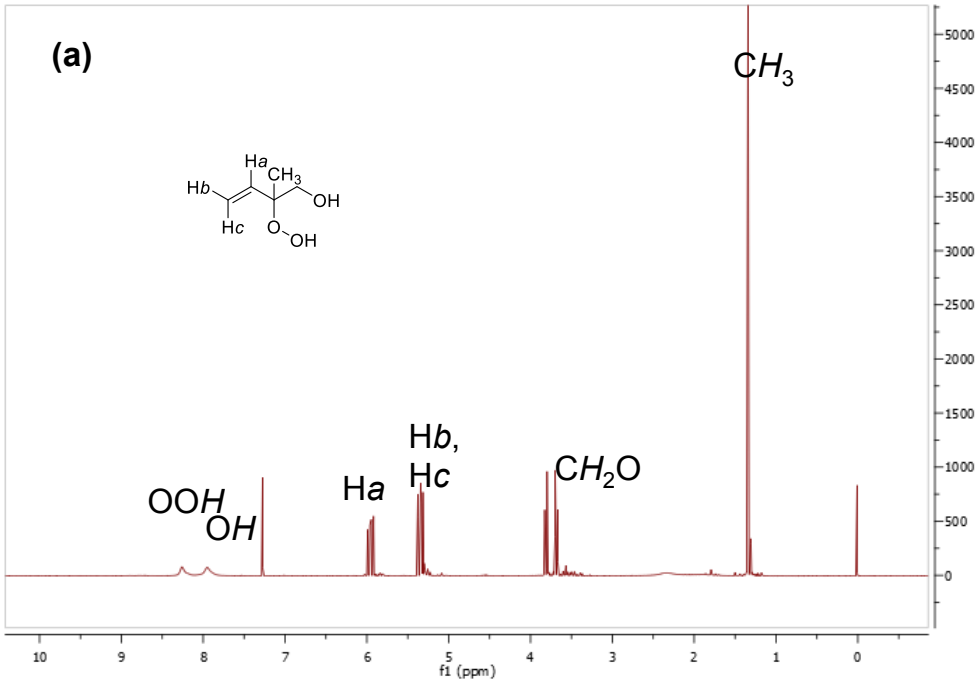

1

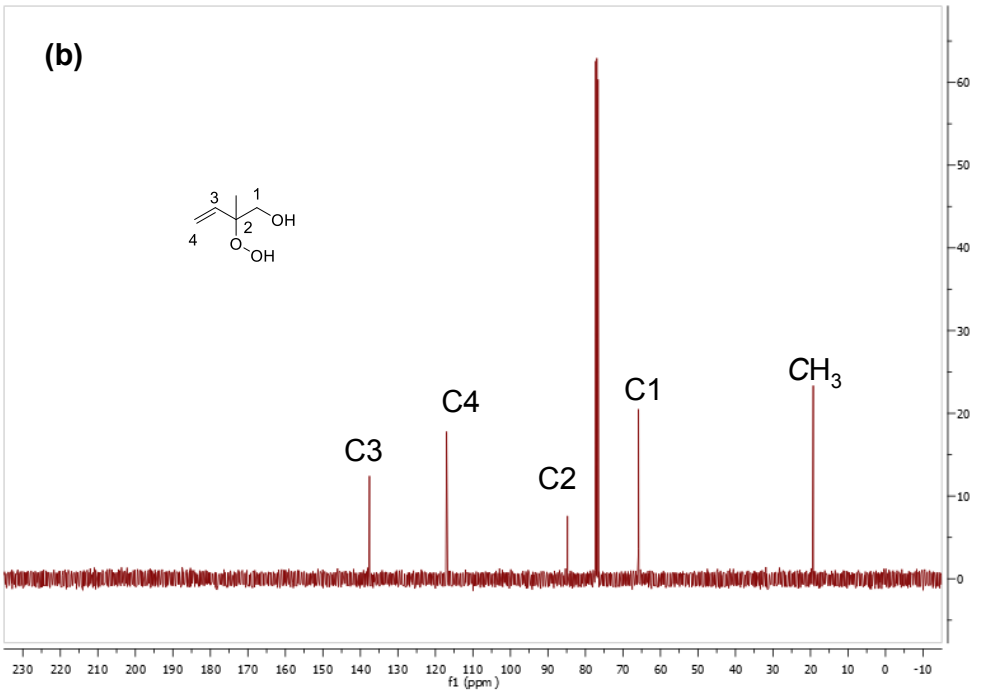

2

3 **Figure S10.** Spectrum of ISOPOOH (2-hydroperoxy-2-methylbut-3-en-1-ol) from (a) ^{1}H
4 NMR (400 MHz, $CDCl_3$); and (b) ^{13}CNMR (100 MHz, $CDCl_3$).

5

6

7

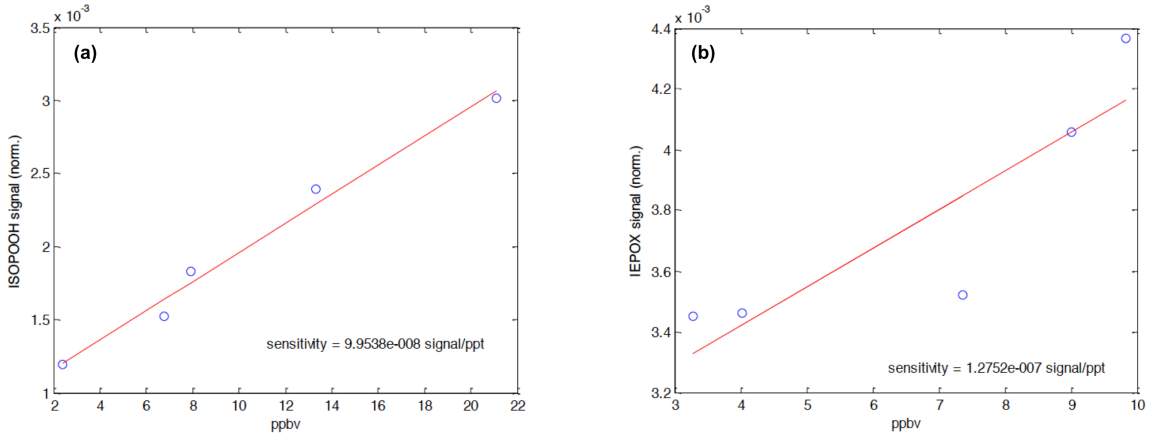

Figure S11. Response factors of CIMS toward (a) ISOPOOH and (b) IEPOX measured after 2013 campaign. IEPOX response factor is lower compared to that measured in 2013. This is likely due to changes in voltages setting and repairs done after 2013 SOAS campaign.

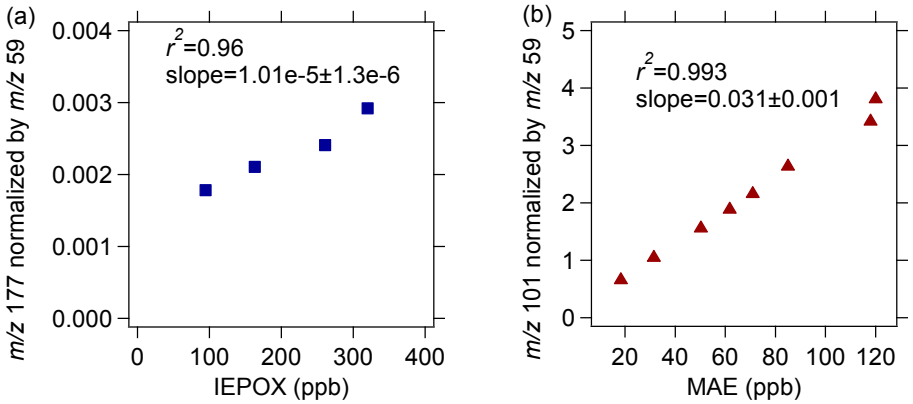

Figure S12. Calibration factors of (a) IEPOX and (b) MAE from HR-ToF-CIMS with acetate ion chemistry conducted before 2013 SOAS campaign.

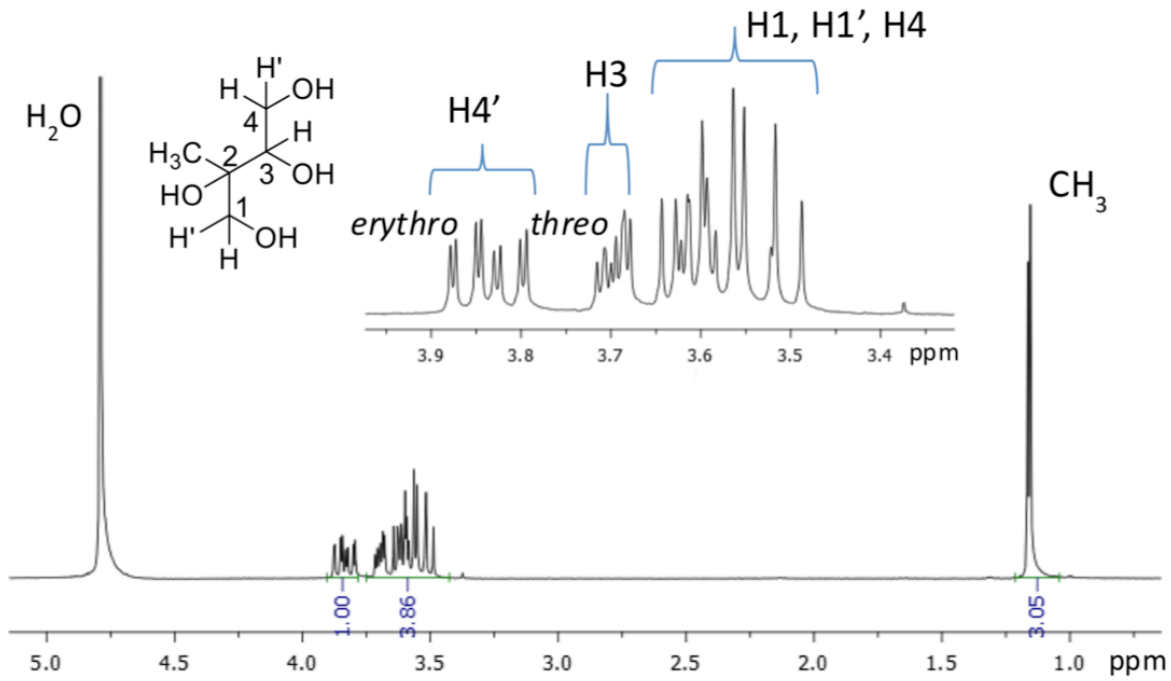

Figure S13. ^{1}H NMR spectrum (D_2O, 400 MHz) of 2-C-methylerythritol and 2-C-methylthreitol mixture.

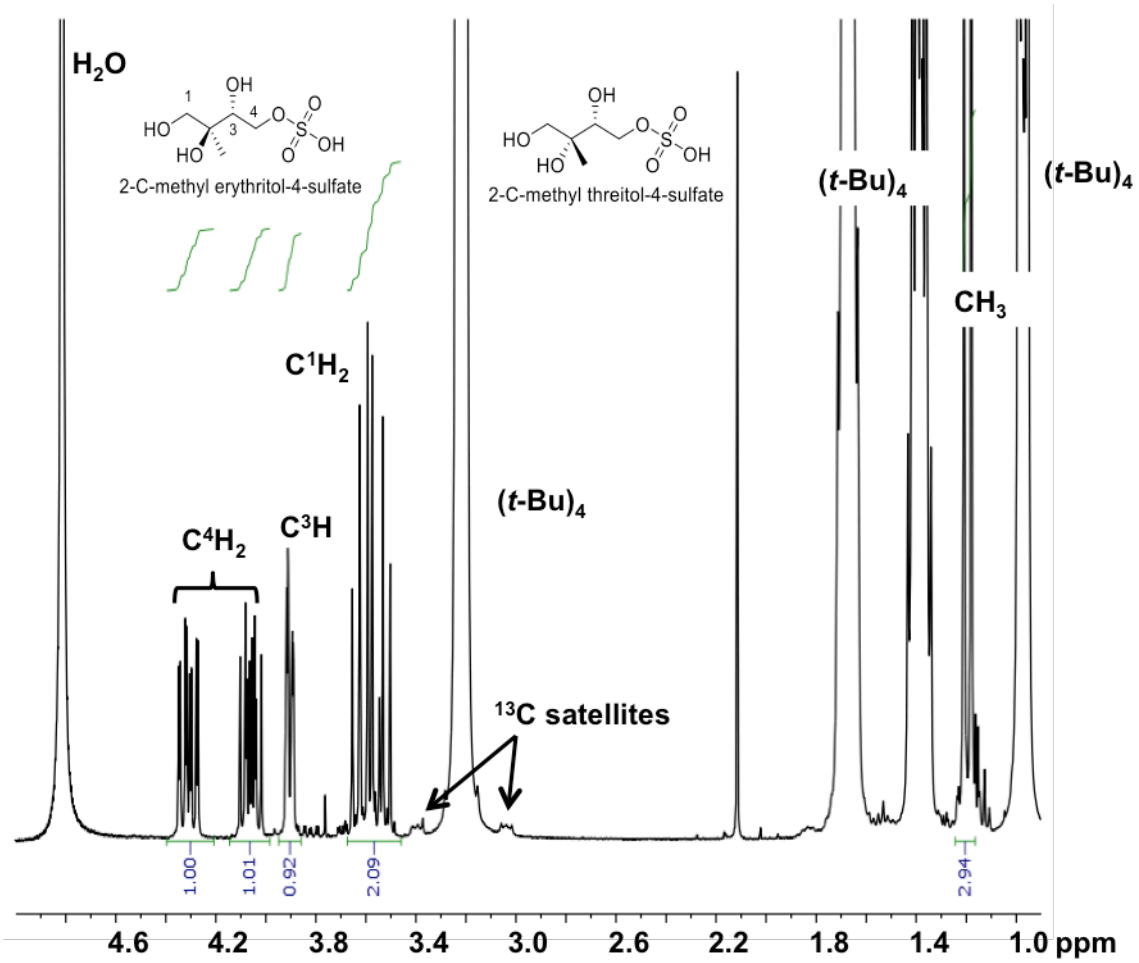

Figure S14. ^{1}H NMR spectrum (D_2O, 400 MHz) of 2-C-methyltetrol sulfate ester mixture.

E. Gas- and Particle-phase Analysis

Table S5. Correlation of PMF Factors with collocated measurements and reference mass spectra.

	IEPOX-OA	LV-OOA	91Fac
r^2 *Time Series*			
CO	0.29	0.38	0.18
NO_x (=NO+NO_2)	0.03	0.00	0.03
NO_y	0.09	0.19	0.16
NO_z	0.08	0.16	0.15
O_x (=NO_2+O_3)	0.07	0.36	0.06
SO_4	0.31	0.23	0.07
ACSM SO_4	0.58	0.39	0.18
ACSM NO_3	0.55	0.62	0.55

	IEPOX-OA	LV-OOA	91Fac
ACSM NH_4	0.47	0.48	0.23
CIMS MAE	0.27	0.30	0.33
CIMS IEPOX	0.24	0.31	0.37
PTR-MS Isoprene	0.01	0.08	0.05
PTR-MS MVK+MACR	0.36	0.37	0.47
PTR-MS Acetonitrile	0.12	0.09	0.07
PTR-MS Monoterpenes	0.00	0.02	0.01
LWC	0.00	0.06	0.00
pH	0.05	0.08	0.02
WSOC	0.37	0.28	0.27
r^2 *Mass Spectra*			
HOA[a]	0.11	0.05	0.24
LV-OOA[a]	0.97	0.97	0.92
SV-OOA[a]	0.55	0.41	0.75
BBOA[a]	0.46	0.28	0.56
82Fac[b]	0.89	0.71	0.82
91Fac[b]	0.54	0.42	0.75
IEPOX-OA[c]	0.81	0.65	0.83
Lab IEPOX SOA[c]	0.55	0.32	0.49

References: (a) Ng et al. (2011), (b) Robinson et al. (2011), and (c) Budisulistiorini et al. (2013)

Table S6. Correlation of isoprene-derived SOA tracers measured by GC/EI-MS and UPLC/DAD-ESI-HR-Q-TOFMS with collocated measurements.

r^2	MeTHF	MeTetrol	Triol	2-MG	IEPOXOS	IEPOXOSdimer	MAEOS
CO	0.07	0.34	0.29	0.45	0.36	0.15	0.25
NO_x (=NO+NO_2)	0.03	0.00	0.01	0.03	0.00	0.04	0.00
NO_y	0.16	0.11	0.12	0.38	0.15	0.02	0.23
NO_z	0.29	0.17	0.23	0.35	0.28	0.12	0.37
O_x (=NO_2+O_3)	0.05	0.01	0.01	0.00	0.04	0.03	0.05
SO_4	0.06	0.36	0.31	0.35	0.34	0.15	0.26
ACSM SO_4	0.09	0.36	0.31	0.31	0.35	0.22	0.31
ACSM NO_3	0.17	0.41	0.38	0.46	0.40	0.32	0.41
ACSM NH_4	0.07	0.32	0.27	0.32	0.30	0.18	0.30
CIMS MAE	0.45	0.26	0.33	0.37	0.31	0.23	0.47
CIMS IEPOX	0.41	0.21	0.28	0.30	0.25	0.19	0.41
PTR-MS Isoprene	0.06	0.03	0.03	0.09	0.09	0.05	0.06
PTR-MS MVK+MACR	0.15	0.24	0.26	0.29	0.32	0.21	0.21
PTR-MS Acetonitrile	0.01	0.20	0.18	0.33	0.30	0.17	0.13
LWC	0.02	0.00	0.01	0.02	0.05	0.02	0.02
pH	0.07	0.05	0.06	0.06	0.13	0.08	0.06

WSOC	0.06	0.33	0.31	0.29	0.40	0.30	0.22

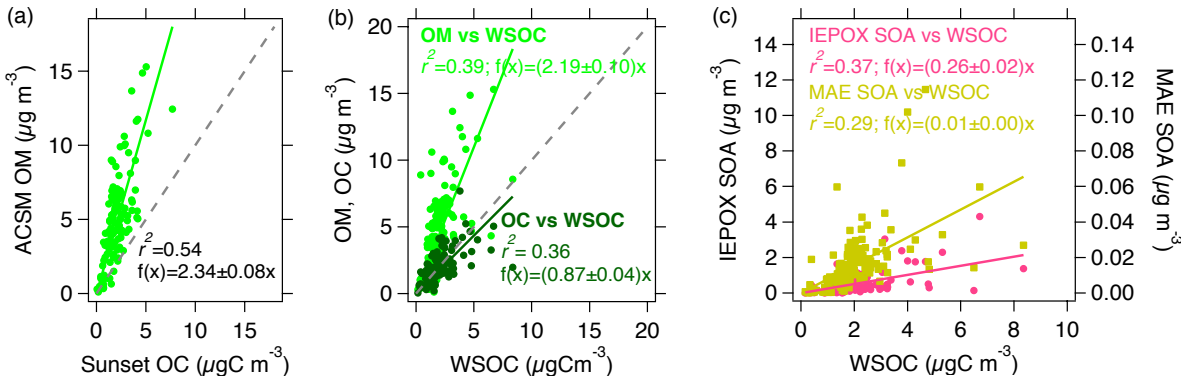

Figure S15. Comparisons of organic matter (OM) by ACSM with organic carbon (OC) by Sunset OC/EC (a) and water soluble organic carbon (WSOC) measurements (b). OM:OC ratio was estimated to be 2.34. Comparisons of WSOC with SOA tracers (c) indicate that IEPOX- and MAE-derived masses might explain 25% and 0.5% of the WSOC mass, respectively.

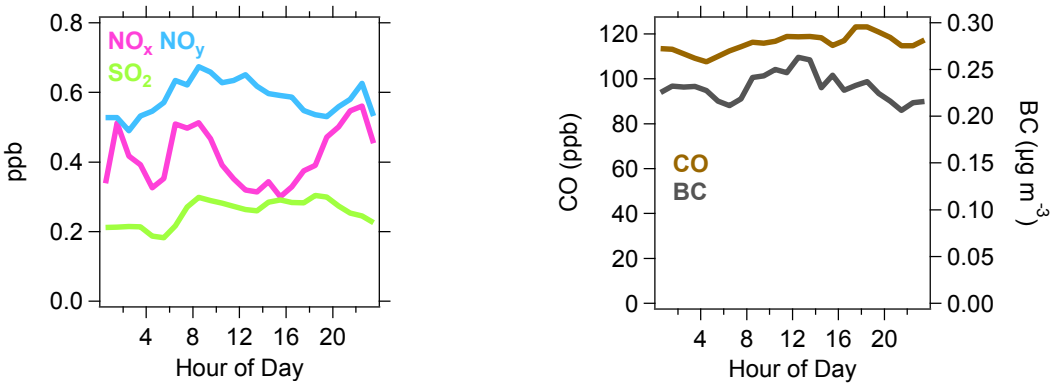

Figure S16. Diurnal variation of NO_x, NO_y, and SO_2 (left) and CO and BC (right). Overall, concentration of primary tracers (i.e., NO_x, SO_2, CO, and BC) are small.

Potential Source of 91Fac

The source of 91Fac is currently a matter of speculation. Aged biomass burning aerosol (Robinson et al., 2011) has been suggested because of the similarity of the profile to that of biomass burning aerosols, except for absence of prominent ions at *m/z* 60 and 73 expected from levoglucosan (Alfarra et al., 2007). A more recent study proposed that fresh BVOC (i.e., monoterpene) oxidation products are a possible source based on chamber experiments (Chen et al., 2014). At LRK, 91Fac correlates moderately with sulfated and nitrated species of monoterpene SOA, i.e., $C_{10}H_{16}O_7S$ (r^2 = 0.37; Fig. 5) and $C_9H_5NO_8S$ (r^2 = 0.41), but weakly with acid species, i.e., terpenylic acid ($C_8H_{12}O_4$, r^2 = 0.36). Good correlation between LRK 91Fac and aerosol nitrate (r^2 = 0.55) and weak association (r^2 < 0.2) with NO_x, NO_y, and CO (Table S5) are indicative of an aged aerosol that may be associated with nitrate radical chemistry or as yet unidentified pathways.

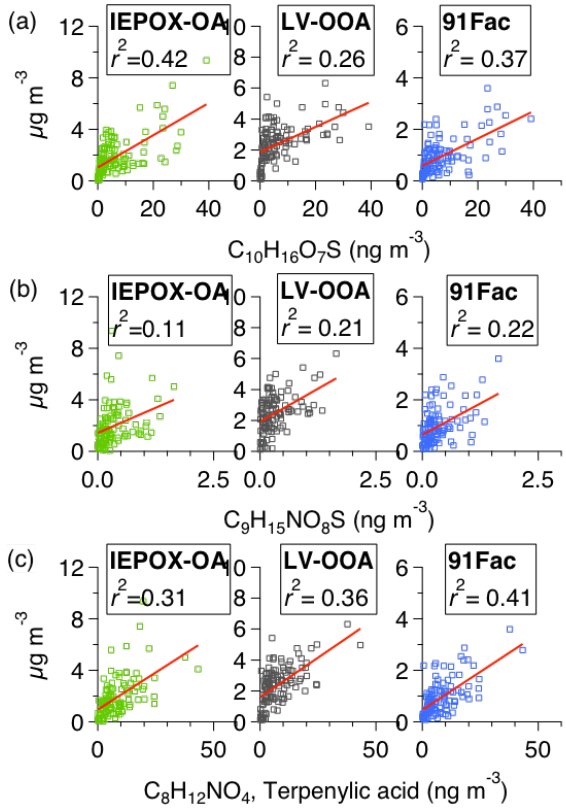

Figure S17. Correlation of PMF factors with α-pinene derived organosulfate, $C_{10}H_{16}O_7S$ (a), nitrated organosulfates, $C_9H_{15}NO_8S$ (b), and terpenylic acid $C_8H_{12}NO_4$ (c).

HYSPLIT model

Atmospheric transport during the 2013 SOAS field study was analyzed by computing air trajectories using the HYSPLIT Model (http://ready.arl.noaa.gov/HYSPLIT.php) from the Air Resources Laboratory of the National Oceanic and Atmospheric Administration (NOAA). Wind fields from the NOAA-NCAR Global Reanalysis data set were used as input to HYSPLIT for trajectory calculations. Vertical air parcel motion was determined from estimated vertical velocities in the input data set. Air trajectories were computed 24 hours backward in time from Look Rock in one-hour time steps with ending heights at Look Rock of 100, 500 and 1500 m above ground level. Each trajectory arrived at Look Rock at midnight (EST) or 01:00 EDT.

To further examine the influence of NO_x emissions as well as aerosol acidity, we examined where air masses originated from to our site using back trajectory (HYSPLIT model) analysis. Figs. S18 and S19 present the back-trajectories of air mass arrived at the LRK site at 01:00 local time (00:00 EST) of the date on each plot. During periods (10 – 16 June 2013) of high levels of IEPOX-derived SOA mass, the model shows that air masses were coming from the south at the beginning and slowly shifted from the west for the next three days (Fig. S18). Throughout periods when IEPOX-derived SOA is low (2 – 8 July 2013), air masses were coming from the south and southeast. Considering that the site is located at about 800 m above sea level, it is less likely that the air masses (at 100 m above the surface) carried NO_x from nearby sources. Air masses at 500 m and 1500 m above the surface might carry some NOx, however, it might have been diluted during the transport.

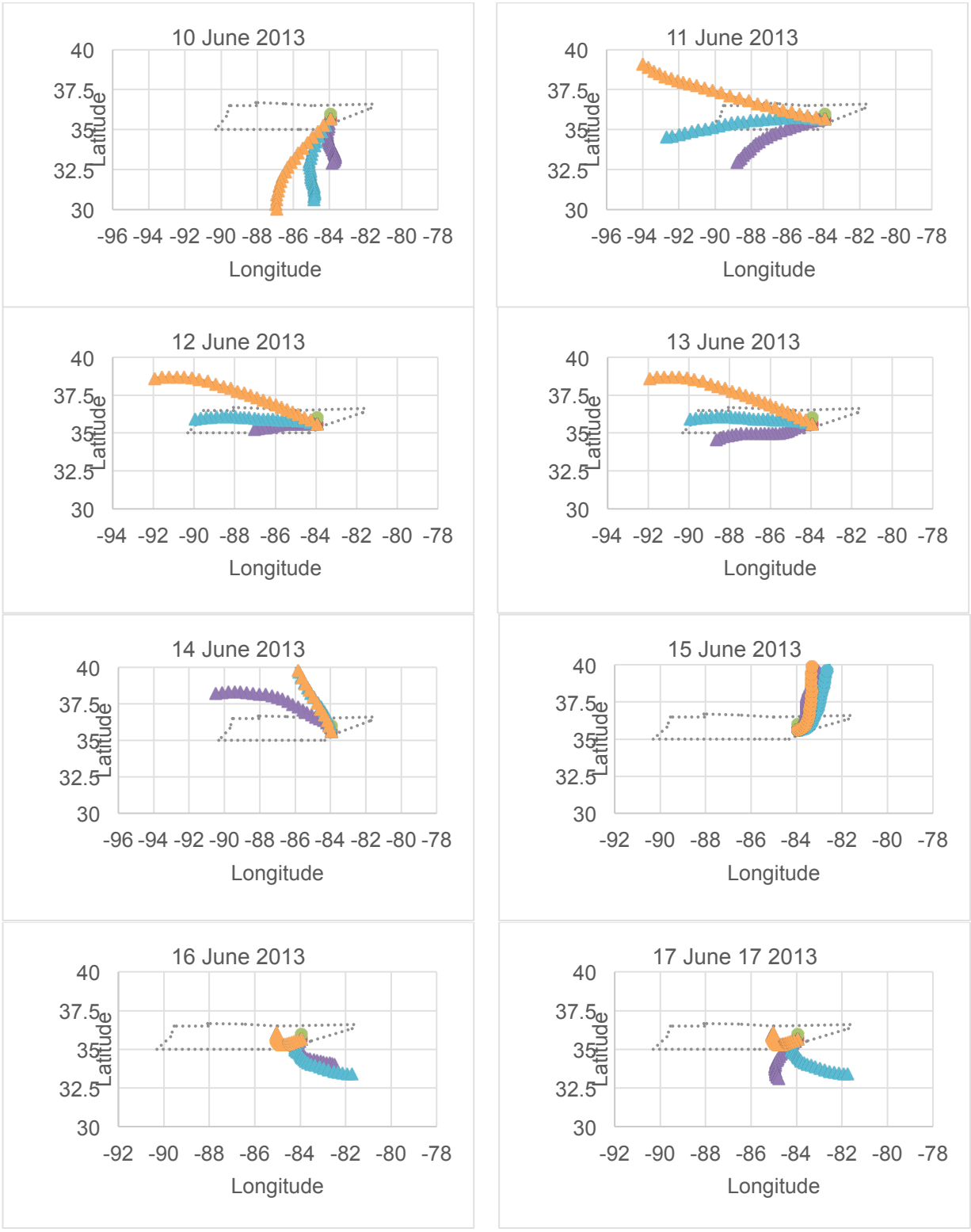

Figure S18. Air mass back trajectories from HYSPLIT 24-hr model during the first and second intensive filter sampling periods when high IEPOX-derived SOA formation was observed. The backtrajectories were estimated at elevation of 100 m (orange), 500 m (turqoise), and 1500 m (purple) above the site. Concentration of IEPOX-derived SOA started to decrease on June 17, 2013.

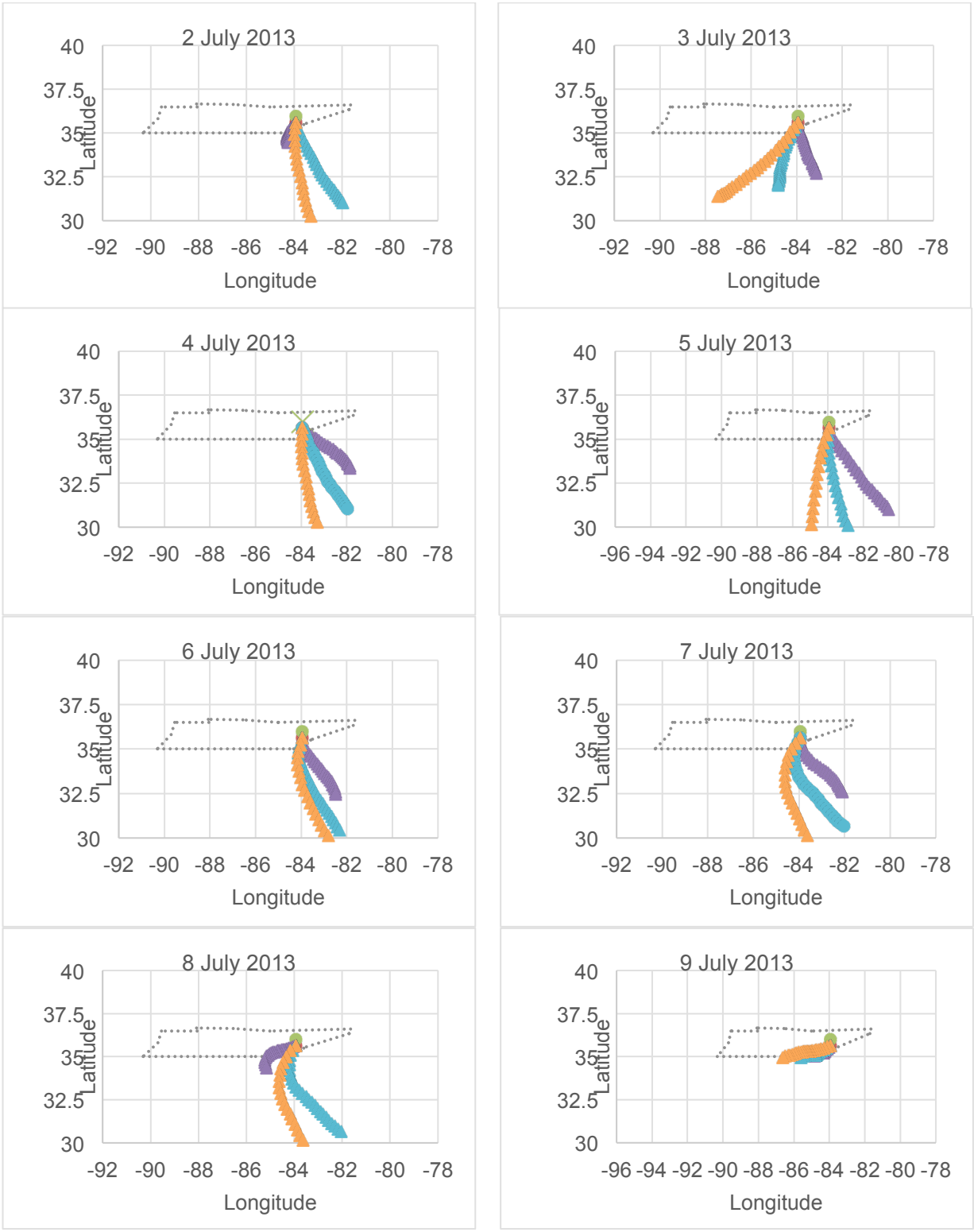

Figure S19. Air mass back trajectories from HYSPLIT 24-hr model during low IEPOX-derived SOA formation of 2 – 8 July 2013. 9 July 2013 was the beginning of the fourth intensive period. The backtrajectories were estimated at elevation of 100 m (orange), 500 m (turqoise), and 1500 m (purple) above the site.

Results from simpleGAMMA

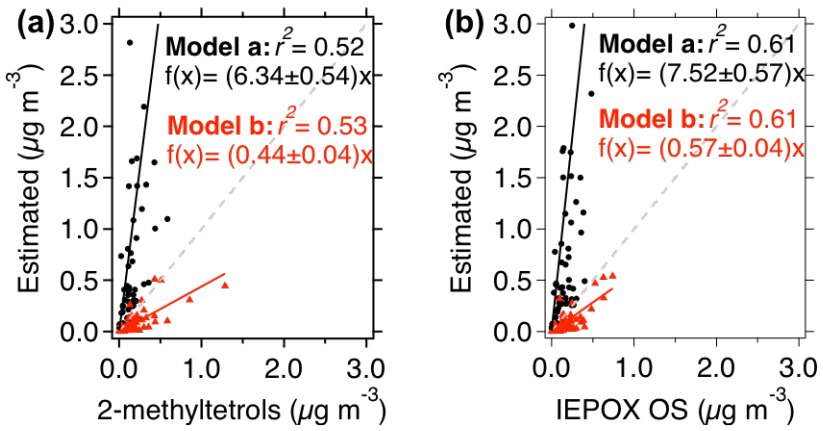

Figure S20. Correlation of (a) 2-methyltetrols and (b) IEPOX-derived organosulfate (IEPOX OS) estimated by simpleGAMMA by assumming H* of 3.0×10^7 (Nguyen et al., 2014) (model a) and 2.7×10^6 (Pye et al., 2013) (model b).